and Dr. Deschamp for kindly placing this machine at his disposal.

*Equipe de Recherche Associée au Centre National de la Rechérche Scientifique.

[1] I. B. Bernstein, Phys. Rev. 109, 10 (1958).
[2] E. R. Ault and H. Ikezi, Phys. Fluids 13, 2874 (1970).
[3] J. P. M. Schmitt, Phys. Fluids 15, 2057 (1972).
[4] Y. Ohnuma, S. Miyake, T. Sato, and T. Watari, Phys. Rev. Lett. 26, 541 (1970).
[5] J. P. M. Schmitt, Plasma Phys. 15, 677 (1973).
[6] A. Hirose, I. Alexeff, and W. D. Jones, Phys. Fluids 13, 2039 (1970).

Effect of a Limiter on Ohmic Discharges in the Heliotron D

K. Uo, S. Morimoto, S. Konoshima, M. Koyama,* and A. Iiyoshi
Plasma Physics Laboratory, Faculty of Engineering, Kyoto University, Uji, Japan
(Received 18 July 1973)

Ohmic discharges with and without a limiter are being studied in the Heliotron D. Without the limiter, we observe longer containment time and lower impurity concentration than with the limiter, and a stable current with the safety factor $q_{0H} \simeq 0.4$ is obtained. With the limiter, strong current fluctuations are observed near rational values of the rotational transform, i.e., $\iota/2\pi = (\iota_F + \iota_{0H})/2\pi \simeq 0.5$ and 1.0.

The existence of the material limiter is one of the difficult problems to be solved in conventional toroidal systems such as the tokamak. Impurities produced by the interaction between the plasma and the limiter cause fast energy loss. We obtained an Ohmic-heating current column isolated from the wall of the vacuum vessel by the separatrix of the Heliotron magnetic field[1] without using a material limiter in the experiment on the Heliotron B.[2] The separatrix region in the helical Heliotron field[1,3,4] is also expected to act as a natural limiter, since the outermost closed magnetic surface is located inside the helical conductor without crossing the wall of the vacuum vessel. Similar methods have been proposed to remove the limiter recently.[5,6] In this paper experimental results are reported about the effect of a limiter on the Ohmically heated plasma. We also describe the effects of the rotational transform and the shear on the current instability.

Details of the machine have been described in earlier papers.[7,8] An $l=2$ helical conductor with a major radius of 108.5 cm is hung inside the vacuum chamber. Because of the short pitch (54.5 cm) and the large minor radius (13 cm) of the winding, we can make both the rotational transform and the shear large. The maximum toroidal field strengths due to the toroidal and helical coils are 5 and 3 kG, respectively. An eight-turn air-core transformer for the Ohmic heating is mounted around the vacuum chamber. Disposition of the coil is arranged to minimize stray flux. A capacitor bank of 20 kJ gives a maximum loop voltage V_L of 60 V. The duration of the discharge is 2 msec. A glow discharge is applied[8] in order to clean the vacuum wall and the helical conductor. Base pressure lower than 5×10^{-8} Torr is attained with an oil-free pumping system. Helium gas is used in most cases. By using various preionization methods (such as an electron gun, electron-cyclotron resonance heating, and radio frequency), we can obtain the Ohmic discharge at filling pressure p_f higher than 3×10^{-5} Torr. The plasma current I_{0H} is measured by Rogowskii coils arranged inside the helical coil. The boundary of the plasma is measured by electrostatic probe. The electron density n_e and the temperature T_e are estimated from microwave interferometry and visible light spectroscopy measurements, respectively. The ion temperature T_i is measured by Doppler broadening. Typical parameters are $I_{0H} \lesssim 12$ kA, $n_e = 10^{12}-10^{14}$ cm^{-3}, $T_e = 10-100$ eV, $T_i = 5-30$ eV and $\beta = 0.003-0.12$.

In order to have closed magnetic surfaces in the helical Heliotron field, it is necessary to apply an appropriate vertical field. The plasma itself produces an effective vertical field which displaces the magnetic surfaces. In the Ohmic-heating experiments, an additional vertical field is produced by the current ring and the stray

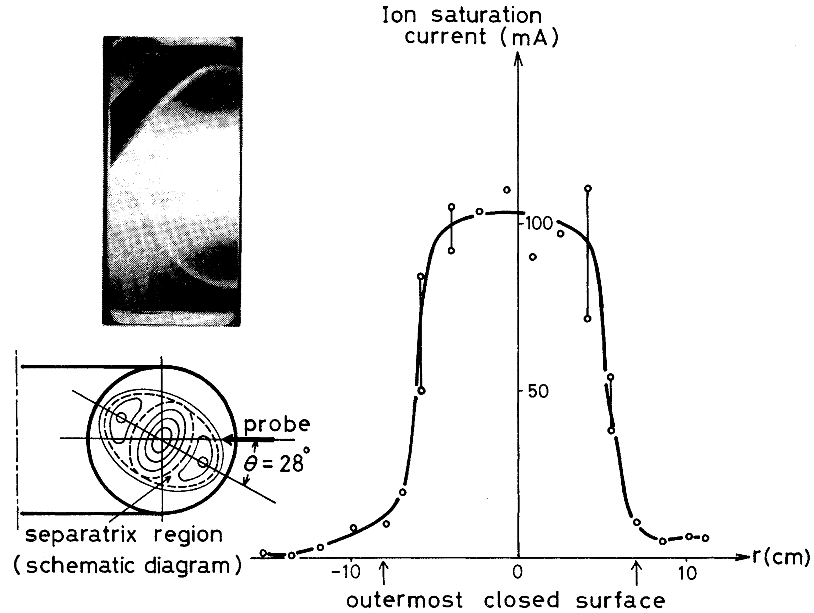

FIG. 1. Schematic drawing of the magnetic surfaces used in the experiment and the radial profile of the ion saturation current during the discharge. The time-integrated photograph of the discharge is superimposed. The limiter is not introduced. $\alpha^* = 0$, $B = 2.05$ kG, $\iota_F \iota_{0H} > 0$.

field of the air-core transformer. Because of the large rotational transform of the Heliotron-D field, however, the displacements of the magnetic surfaces are small, and equilibrium of the current column is easily attained. In the experiments described below, the vertical field which gives a maximum current is applied.

A comparative study of Ohmic heating with and without the limiter is carried out in the field configuration of $\alpha^* = B_{t0}/B_{h\varphi 0} = -0.2$, where B_{t0} and $B_{h\varphi 0}$ are the magnetic flux density of the field produced by the toroidal coil and the longitudinal component on the axis of the field produced by the helical coil, respectively. For magnetic fields of smaller α^*, e.g., $\alpha^* = 0$ and -0.2, the rotational transform of the vacuum field $\iota_F/2\pi$ and the shear parameter Θ are very large near the separatrix ($\iota_F/2\pi = 2.0$ and $\Theta \simeq 0.3$ for $\alpha^* = -0.2$), and the outermost closed magnetic surfaces are relatively small. The observed plasma column is well isolated from the conductor and the wall as shown in Fig. 1. The experimental conditions such as α^*, B, V_L, and p_f are kept constant for both cases, with and without the limiter. The circular-aperture limiter (radius $a_L = 7$ cm) is placed just outside the plasma column so the average plasma radius a_p is nearly equal to that without the limiter. Some parameters of the plasma obtained for a relatively small V_L are shown in Table I. While the input power P_{in} is almost constant, the electron density and the temperature are different by a factor of 2–3. A rough estimation shows that the energy confinement time τ_E is improved by a factor of 4–5 in the discharge without the limiter. The intensities of the impurity lines are considerably reduced by removing the limiter.

The maximum plasma current I_M increases

TABLE I. Parameters of the plasma with and without the limiter.

	I_{0H} (kA)	V_L (V)	P_{in} (kW)	$\bar{n}_e$ (cm^{-3})	T_e (eV)	T_i (eV)	β (%)	τ_E (μsec)[a]	Impurity levels (arbitrary unit) C II(4267 Å)	C III(4647 Å)	O II(4415 Å)
With limiter	1.2	20	28	0.7×10^{13}	20	6	0.6	150	6	6	4
Without limiter	1.3	20	30	1.7×10^{13}	38	12	3	700	1	1	0.1

[a] $\tau_E \equiv W$(total kinetic energy of the plasma)$/P_{\text{in}}$.

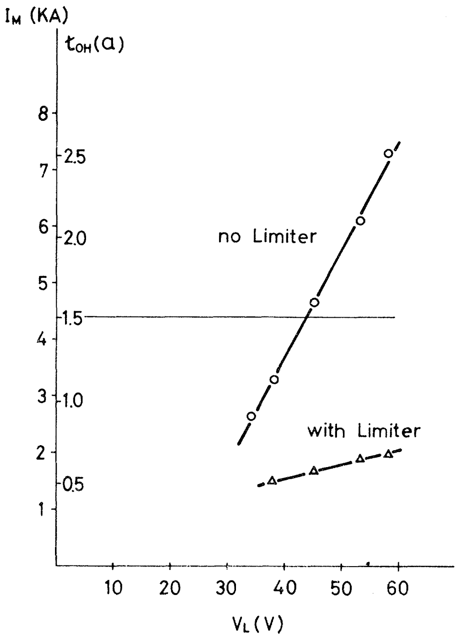

FIG. 2. Maximum plasma current I_M versus the loop voltage V_L at $I_{0H}=I_M$. The experimental conditions are the same for both cases except for the presence of the limiter. $\alpha^*=-0.2$, $B=1.3$ kG, and $\iota_F\iota_{0H}>0$. The mean radius of the plasma is nearly the same for both cases. The line $\iota_{0H}(a)/2\pi=1.5$ is the stability limit for the kink mode calculated according to Ref. 11 assuming a uniform current distribution.

linearly as the loop voltage increases as shown in Fig. 2. The installation of the limiter noticeably reduces the plasma current. In the case without the limiter, instabilities are not observed in I_{0H}, $\dot{I}_{0H}$, and V_L, as shown in Fig. 3(a). The safety factor due to the plasma current $q_{0H}(a_p)$ exceeds the theoretically predicted value for the kink mode[9] which takes into account the shear of the magnetic field. The minimum $q_{0H}(a_p)$ obtained so far is 0.4 and is limited by the available loop voltage. It is not clear whether such a small $q_{0H}(a_p)$ is due to the configuration of the magnetic field or the existence of low-density plasma outside the plasma column.

For smaller ι_F and Θ, i.e., $\iota_F(a)/2\pi=0.2-1.0$ and $\Theta=0.02-0.15$, though these conditions are only obtained by introducing the limiter and adopting larger α^*, i.e., $\alpha^*=0-1.5$, strong fluctuations are observed in the plasma current. When $\iota_F(a_L)/2\pi=0.2-0.3$, the current begins to fluctuate at a certain value of $I_{0H}=I_{0H}^*$ and does not grow any more, as shown in Fig. 3(b). As $\iota_F(a_L)$ is increased the current start to fluctuate at smaller I_{0H}^* than before, but then overcomes the fluctuation reaching a peak value I_M as shown in Fig. 3(c). The strength of the fluctuation reduces as ι_F and Θ are increased. In Fig. 4, I_{0H}^* and I_M are plotted against $\iota_F(a_L)$ and Θ. The current fluctuation begins in the vicinity of a line $[\iota_F(a_L)+\iota_{0H}(a_L)]/2\pi=0.5$, where ι_{0H} is the rotational transform produced by I_{0H}. Except for $\iota_F(a_L)/2\pi \simeq 0.2$ where the instability is very strong, the value of I_M is increased by the increase of V_L. For $\iota_F(a_L)/2\pi \gtrsim 0.5$ we do not observe I_{0H}^* and I_M as the continuation of the former series. Instead, we observe a new series of the instability on the line $[\iota_F(a_L)+\iota_{0H}(a_L)]/2\pi=1$, and it repeats qualitatively the same behavior as before with the further increase of $\iota_F(a_L)$. It is also found that I_{0H}^* is proportional to B. These results suggest that the fluctuation and the limitation of the current are due to the kink instability.[10,11] Qualitative agreement is found between the experiment and the theory of the kink mode.[9] Quantitatively, however, the experimental results for I_{0H}^* are lower than the theoretical values except for the

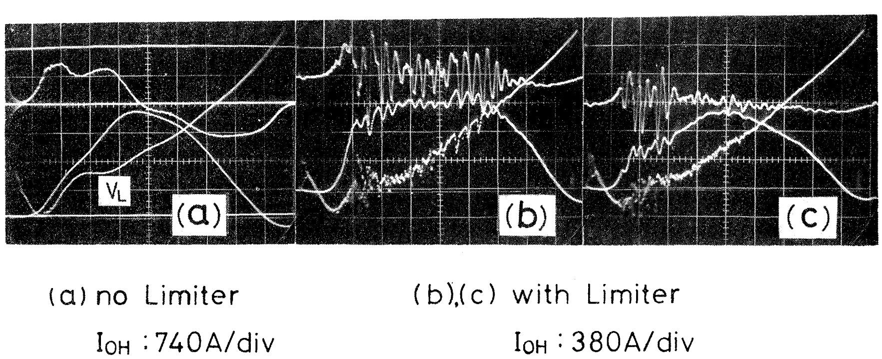

FIG. 3. Oscillograms showing V_L, I_{0H}, and its time derivative $\dot{I}_{0H}$. $B=1.7$ kG, $\iota_F\iota_{0H}>0$, $V_L=10$ V/div, time scale $=0.2$ msec/div. (a) $\alpha^*=-0.2$. (b) $\alpha^*=1.2$, $\iota_F(a_L)/2\pi=0.26$, $\Theta=0.026$. (c) $\alpha^*=0.6$, $\iota_F(a_L)/2\pi=0.45$, $\Theta=0.045$.

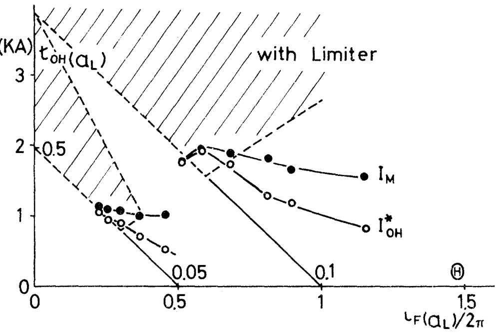

FIG. 4. Rotational transform of the vacuum field at the limiter edge $\iota_F(a_L)$ versus the fluctuation onset current I_{0H}* and the maximum current I_M. The ordinate is also expressed in terms of the rotational transform produced by the current at the limiter edge $\iota_{0H}(a_L)$. The hatched region indicates the theoretically unstable region for a uniform current distribution. $B=1.7$ kG, $V_L \simeq 40$ V.

cases of $\iota_F(a_L)/2\pi \simeq 0.2$ and 0.5 as shown in Fig. 4, where the hatched regions indicate the unstable regions of the theory. A similar phenomenon was observed in the Stellarator C with the $l=3$ winding.[9] Another feature of the experimental results is that the instability for $[\iota_F(a_L)+\iota_{0H}(a_L)]/2\pi \lesssim \frac{1}{3}$ is not observed appreciably. This result is different from the experimental results obtained on the Wenderstein-IIb which has almost no shear.[12]

The authors would like to express their appreciation to Mr. S. Yoshioka, Mr. I. Ohtake, Mr. M. Sato, and Mr. M. Yamada for their assistance throughout the experiment.

*On leave from Chiba Institute of Technology, Chiba, Japan.

[1]K. Uo, J. Phys. Soc. Jap. 16, 1380 (1961).

[2]K. Uo, A. Mohri, H. Oshiyama, R. Kato, and K. Ishii, Phys. Fluids 5, 1293 (1961).

[3]K. Uo, R. Itatani, A. Mohri, H. Oshiyama, S. Ariga, and T. Uede, in *Proceedings of the Third International Conference on Plasma Physics and Controlled Nuclear Fusion Research, Novosibirsk, U.S.S.R., 1968* (International Atomic Energy Agency, Vienna, Austria, 1969), Vol. I, p. 217.

[4]K. Uo, Plasma Phys. 13, 243 (1971).

[5]G. Gourdon, D. Marty, E. K. Maschke, and J. Touche, Nucl. Fusion 11, 161 (1971).

[6]C. Colven, A. Gibson, and P. E. Stott, in *Proceedings of the Fifth European Conference on Controlled Fusion and Plasma Physics, Grenoble, France, 1971* (Service d'Ionique Générale, Association EURATOM–Commissariat à l'Energie Atomique, Centre d'Etudes Nucléaires de Grenoble, Grenoble, France, 1972), Vol. I. p. 6.

[7]K. Uo, A. Iiyoshi, S. Yoshioka, T. Ishida, S. Konoshima, and M. Sato, in *Proceedings of the Fourth International Conference on Plasma Physics and Controlled Nuclear Fusion Research, Madison, Wisconsin, 1971* (International Atomic Energy Agency, Vienna, Austria, 1972), Vol. III, p. 109.

[8]K. Uo, A. Iiyoshi, S. Morimoto, A. Sasaki, S. Yoshioka, I. Ohtake, S. Konoshima, M. Sato, M. Koyama, and T. Obiki, in *Proceedings of the Third International Symposium on Toroidal Plasma Confinement, Garching, Germany, 1973* (Max-Planck-Institut für Plasmaphysik, Garching, Germany, 1973), D5.

[9]R. M. Sinclair, S. Yoshikawa, W. L. Harries, K. M. Young, K. E. Weimer, and J. L. Johnson, Phys. Fluids 8, 118 (1965).

[10]J. L. Johnson, C. R. Oberman, R. M. Kulsrud, and E. A. Frieman, Phys. Fluids 1, 281 (1958).

[11]M. D. Kruskal, J. L. Johnson, M. B. Gottlieb, and L. M. Goldman, Phys. Fluids 1, 421 (1958).

[12]G. Grieger, R. Jaenicke, C. O. L. Juulman, C. Mahn, H. Renner, H. Ringler, G. Schilling, G. H. Wolf, and J. Hugill, Plasma Phys. 15, 151 (1973).

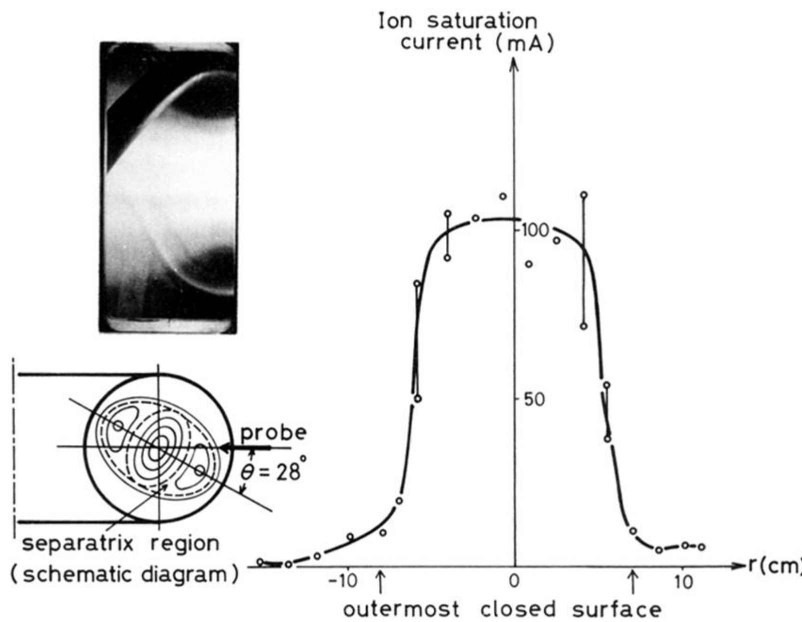

FIG. 1. Schematic drawing of the magnetic surfaces used in the experiment and the radial profile of the ion saturation current during the discharge. The time-integrated photograph of the discharge is superimposed. The limiter is not introduced. $\alpha^* = 0$, $B = 2.05$ kG, $\iota_F \iota_{0H} > 0$.

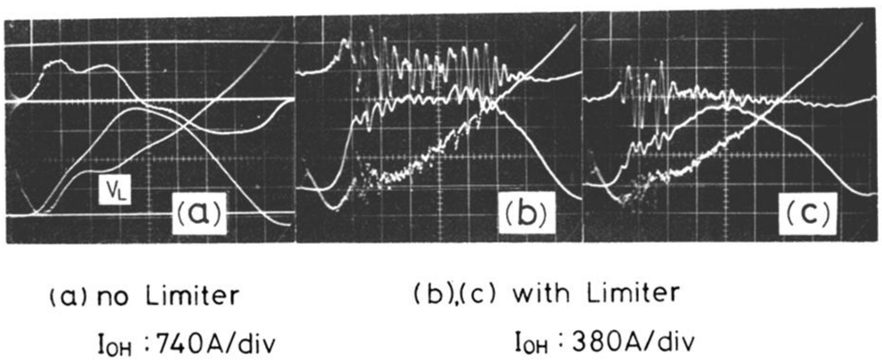

FIG. 3. Oscillograms showing V_L, I_{0H}, and its time derivative $\dot{I}_{0H}$. $B = 1.7$ kG, $\iota_F \iota_{0H} > 0$, $V_L = 10$ V/div, time scale = 0.2 msec/div. (a) $\alpha^* = -0.2$. (b) $\alpha^* = 1.2$, $\iota_F(a_L)/2\pi = 0.26$, $\Theta = 0.026$. (c) $\alpha^* = 0.6$, $\iota_F(a_L)/2\pi = 0.45$, $\Theta = 0.045$.